Published in final edited form as:
J Immunol. 2012 December 15; 189(12): 5820–5830. doi:10.4049/jimmunol.1201514.

Molecular characterization of the early B cell response to pulmonary *Cryptococcus neoformans* infection

Soma Rohatgi[*] and **Liise-anne Pirofski**[*,†]

[*]Division of Infectious Diseases, Department of Medicine, Albert Einstein College of Medicine & Montefiore Medical Center, Bronx, NY 10461, USA

[†]Department of Microbiology and Immunology, Albert Einstein College of Medicine, Bronx, NY 10461, USA

Abstract

The role of B cells in host defense against fungi has been difficult to establish. We quantified and determined the molecular derivation of B-1a, B-1b and B-2 B-cell populations in C57BL/6 mice after pulmonary infection with *Cryptococcus neoformans* (CN). Total B-1 and B-2 cell numbers increased in lungs and peritoneal cavity (PerC) as early as day one post-infection, but lacked signs of clonal expansion. Labeled capsular (24067) and acapsular (Cap67) CN strains were used to identify CN-binding B-cell subsets by flow-cytometry. PerC B-1a B cells exhibited the most acapsular and capsular CN-binding in CN-infected mice and CN-selected B-1 B cells secreted laminarin- and CN-binding IgM. Single-cell PCR-based sequence analysis of B-1a, B-1b and B-2 cell immunoglobulin heavy chain variable region (V_H) genes revealed increased usage of V_H11 and V_H12, respectively, in acapsular and capsular CN-selected B-1a cells. Germline V_H segments were used with capsular CN-selected cells having less junctional diversity than acapsular CN-selected cells. Further studies in B-1 B cell-depleted mice showed that these mice had higher brain and lung fungal burdens and less alveolar macrophage phagocytosis of CN than control and B-1a B cell-reconstituted mice. Together, these results establish a mechanistic role for B-1 B cells in the innate B-cell response to pulmonary infection with CN and reveal that IgM-producing B-1a cells, which express germline V_H genes, bind CN and contribute to early fungal clearance. Thus, B-1a B cells provide a first line of defense during pulmonary CN infection in mice.

Introduction

The crucial factor determining the outcome of *Cryptococcus neoformans* (CN) infection is the immune status of the host, with cryptococcal disease occurring most commonly in those with impaired immunity, particularly HIV/AIDS-associated CD4 T cell deficiency. The central importance of T cells in host defense against CN has been established in murine models (1, 2); however, the role of B cells has not been definitively established. Multiple laboratories have demonstrated that monoclonal antibodies (mAbs) to the CN capsular polysaccharide glucuronoxylomannan (GXM) can protect mice against lethal CN infection (3–7) by a variety of mechanisms (8–14). GXM-binding murine mAbs generated from the adaptive response to GXM, are derived from a highly restricted B cell repertoire expressing the immunoglobulin variable region heavy chain (V_H) gene 7183 (15, 16). Similarly, human GXM-binding mAbs use V_H3 genes with structural homology to mouse 7183 genes (17, 18). As V_H3 genes are depleted in HIV infection, it has been hypothesized that a hole in antibody repertoire could increase susceptibility to cryptococcosis (19).

Contact Information: l.pirofski@einstein.yu.edu, Telephone: 718-430-2940, Fax: 718-430-8968.

The sequences presented in this article have been submitted to GenBank under accession numbers Bankits: JX120180 - JX120361.

In addition to V_H3-expressing B cells, IgM memory ($CD27^+IgM^+IgD^-$) B cells are also depleted in HIV infection (20). IgM memory B cells produce 'naturally occurring' IgM (21) that has an intrinsic ability to bind conserved microbial determinants, such as α- and β-glucans, which are present in most fungal cell walls (22). As natural IgM is produced in the absence of antigen stimulation, it is a part of the innate immune system that is considered to provide ready-made pathogen defense (23). It has previously been shown that peripheral blood IgM memory B cell levels were lower in HIV-infected individuals who developed CN than those who did not (24) and that HIV-infected individuals have lower levels of serum GXM-binding IgM than HIV-uninfected individuals (25, 26). In mice, IgM deficiency was associated with increased susceptibility to pulmonary CN infection and a reduced level of alveolar macrophage phagocytosis of CN that increased after reconstitution with natural mouse (non-immune) IgM (27). Natural mouse IgM bound to β-1,3 glucans on *Pneumocystis* and *Aspergillus fumigatus* and enhanced immunity to *Pneumocystis* (22). Further, a natural mAb to keratin protected mice against *Candida albicans* (28) and mAbs to laminarin (a β-1,3 glucan) bound to *Candida albicans* and *Cryptococcus neoformans* and protected mice from lethal infection with these fungi (14, 29).

Although soluble GXM-elicited mAbs protect mice against CN, the question of whether or not B cells contribute to host defense against CN is unresolved. One study found no difference in CN lethality in B cell depleted and B cell sufficient mice (30), while another linked resistance to CN in T cell deficient mice to B cells (31). B cells were the predominant cell type in the lungs of immunocompetent CN-infected mice (32) and pulmonary CN was more lethal in B cell-deficient than B cell-sufficient and *xid* mice (33, 34). The latter lack B-1 B cells and natural IgM, suggesting a beneficial role for these constituents in protection against CN.

Mature B cells can be classified into follicular B, marginal zone B, and B-1 B cells; with follicular and marginal zone B cells being commonly referred to as B-2 cells (35). B-1 B cells consist of B-1a and B-1b subsets, which are distinguished by surface expression of CD5 (36). B-1 B cells ($CD19^{hi}B220^{lo}IgM^{hi}IgD^{lo}$) differ from the B-2 B cells ($CD19^{lo}B220^{hi}IgM^{lo}IgD^{hi}$) in their capability to self-renew (37). B-1 B cells, which are the source of natural IgM and considered a homolog of human IgM memory B cells in mice (38), reside predominantly in the pleural and peritoneal cavities, but are also present in the spleen (23). These cells can also migrate to sites of inflammation, differentiate into mononuclear phagocytes (39), and have been shown to kill CN *in vitro* (40). Recently, resistance of B cell deficient (uMT) mice to *Aspergillus fumigatus* was linked to the discovery of B-1 B cells in these mice (41). Although B-1 cells have been linked to anti-fungal activity against CN (40, 42), their role in host defense has not been formally established.

In this study, we analyzed the mouse B cell response to pulmonary CN infection and the V_H repertoire of CN-selected and unselected B-1 and B-2 B cell populations. Our data show that peritoneal cavity B-1a B cells had the most CN-binding cells. CN-selected B-1 cells secreted IgM that bound to laminarin and CN cells, and used highly restricted V_H11 and V_H12 genes that are known to confer specificity for phosphatidyl choline (PtC). A mechanistic role for B-1 B cells was established in B-1 B cell depleted mice, which had higher lung and brain fungal burdens and less alveolar macrophage phagocytosis of CN than control and B-1a B cell reconstituted mice. In summary, our findings reveal a role for B-1a B cell subset during pulmonary CN infection in mice.

Materials and Methods

Mice

Six to eight week old C57BL/6 mice obtained from National Cancer Institute (Charles River Laboratories) and housed in the Institute for Animal Studies of the Albert Einstein College of Medicine were used. All mouse experiments were conducted with prior approval from the Animal Care and Use Committee, following established guidelines.

CN strains and inocula for infection

Serotype D CN, strain 24067 (American Type Culture Collection (ATCC)), extensively used in mice to study immunity to CN (43, 44) was used. GFP labeled 24067 was provided by Dr. A. Alspaugh (Duke University) and acapsular Cap67 (ATCC 52817) was provided by Dr. A. Casadevall (Albert Einstein College of Medicine). Cap67 was labeled with 10 μg/ml of Uvitex 2B dye (Polysciences Inc., Eppelheim). For some experiments, CN was heat-killed at 65°C for 30 min. CN cultures were grown in Sabouraud dextrose broth (Becton Dickinson) for 52 to 56 h at 37°C with agitation. Mice were infected intranasally (*i.n*) with 5×10^5 CFU of unlabeled 24067 in 20 μl of PBS as described (27).

BrdU staining

For BrdU assays, CN-infected and PBS-treated C57BL/6 mice were injected intraperitoneally (*i.p.*) with 1 mg of BrdU one day prior to tissue harvest. At indicated times, mice were killed, and cells from various tissues were harvested. A BrdU flow kit (BD Biosciences) was used as directed to assess BrdU uptake by flow cytometry.

Cell purification, FACS staining and CN-binding

For isolation of cells from lungs, spleen and mediastinal lymph nodes (medLN), tissue were homogenized using a gentle-MACS dissociator (Miltenyi Biotec.), following the manufacturer's instructions. Peritoneal cavity (PerC) cells were obtained by flushing the peritoneum with saline. Erythrocytes were lysed in RBC lysis buffer. The isolated cells were filtered, resuspended in 1% BSA-PBS and counted.

CN-binding in PerC B cell subsets was detected by flow-cytometry based on a previously published method (45). Aliquots of mouse cells (10^6) were incubated with 10^7 CFU of heat-killed Uvitex-labeled Cap67 or GFP-expressing 24067 and washed twice with PBS. After blocking with rat anti-mouse CD16/32, immuno-staining was performed at 4°C for 20 min in 1% BSA-PBS using a cocktail of: CD19-PE-Cy7, B220-APC-Cy7, IgD-APC, CD5-PE, and IgM-PerCP (BD Biosciences). Single-color controls and fluorescence-minus one controls were included to ensure proper gating. B cell populations were defined as Total B: $CD19^+$; B-2: $CD19^{lo}B220^{hi}IgD^{hi}IgM^{lo}$; B1: $CD19^{hi}$ $B220^{int}IgD^{int}IgM^{hi}$; B-1a: $CD19^{hi}B220^{int}IgD^{int}IgM^{hi}CD5^+$; B-1b: $CD19^{hi}B220^{int}IgD^{int}$, $IgM^{hi}CD5^-$. Data was collected on a BD LSR II (Becton Dickinson) flow-cytometer. A total of 100,000 events per sample were analyzed. All analyses were performed using FlowJo (TreeStar, Ashland).

ELISPOT

IgM secretion and CN antigen binding of B cells was determined by ELISPOT assay as previously described (46). MultiScreen HA membrane plates (Millipore) were coated with goat anti-mouse IgM (5 μg/ml), heat-killed Cap67 and 24067 (10^7 CFU), Laminarin (Sigma) (10 μg/ml), and GXM (10 μg/ml), purified as described (47) in PBS and incubated overnight at 4°C. Plates were blocked with 1% BSA-RPMI for 2 h at 37°C. Isolated splenic/PerC/lungs/medLN cells (ranging from 10^5/well to 10^2/well) from CN-infected mice were added to the plate and incubated for 16 h at 37°C, 5% CO_2. B-1a and B-1b cells were pooled

together and assayed as B-1 fraction, due to small numbers of CN-selected cells in ELISPOTs testing specificity of CN-selected cells. After incubation, cells were discarded and biotinylated anti-mouse IgM Ab (1:5000, Southern Biotech) was added for 2 h at 37°C, followed by Streptavidin-HRP (1:100, BD Biosciences) for 1 h at room temperature. Substrate 3-amino-9-ethylcarbazole (BD Biosciences) was added for 30 min at room temperature. Color development was stopped with water and plates were dried overnight. Spots were counted using ELISPOT reader (Autoimmun Diagnostika).

Single cell sorting of CN-binding B-cell subsets

B-1a, B-1b and B-2 cells identified as capsular (GFP-24067) or acapsular (Uvitex Cap67) CN-binding populations by FACS were isolated by sorting and referred to as CN-selected populations. A separate aliquot of B cells stained with unlabeled capsular or acapsular CN was used to determine gating for CN-selected cells. CN-selected and unselected B-1a, B-1b and B-2 cells were purified using FACSAria cell sorter (BD Biosciences) and collected as single cells directly in 96-well PCR plates containing 4 μl of ice cold lysis buffer (0.5X endonuclease free PBS supplemented with 10 U of RNAse Inhibitor) on dry ice, using established procedures (48, 49). A no-cell control was included in each plate. Single B cells were sorted according to surface marker expression patterns applying FSC-H/FSC-W-based duplet discrimination and single cell sort mask settings. Post-sort re-analysis of the B cell subpopulations by FACS revealed ≥ 98% purity.

Single cell RT-PCR and Ig gene amplification

cDNA was synthesized from sorted single B cells in a final volume of 20 μl in the original 96-well sorting plate. Pooled heavy chain constant region specific RT primers were used at a final concentration 0.15 μM each. The RT primers used, reaction composition and cycling conditions were as previously described (50). IgH V gene transcripts were amplified by touchdown nested PCR using 5 μl of unpurified cDNA as template. The 5′ IgV_H family-specific external and internal primer-mixes, 3′ C_H primers, reaction compositions and cycling parameters used for nested PCRs were as reported (50). The amplified products were analyzed on a 1% agarose gel.

Sequencing and Sequence Analysis of the Ig V_H regions

RT-PCR amplified products were column purified (Qiagen) and sequenced directly (Genewiz) using a 3′ J_H antisense primer, as previously described (50). Sequences were analyzed using MacVector (with Assembler) software (version 12.0.2: MacVector Inc). Ig gene/family assignment for the expressed V_H genes was done using IMGT (ImMunoGeneTics; www.imgt.org/) and IgBLAST (www.ncbi.nlm.nih.gov/igblast/) germline databases. FR/CDR assignments and codon numbering were according to the Kabat system. Sequence analysis was restricted to the sequence internal to the 5′ and 3′ internal primers. The D_H genes were assigned as previously described, wherein at least five nucleotides had to match germ line D_H gene sequence (51). Any nucleotides that could not be assigned to a coding sequence or P addition were considered N nucleotides.

Accession Numbers

The nucleotide sequences of the Ig genes expressed by the single cells listed in Sup Table I have been deposited in GenBank (www.ncbi.nlm.nih.gov/GenBank/index.html). The following accession numbers were provided, Bankits: JX120180-JX120361.

B-1 cell depletion

Since B-1 cells circulate within peritoneal and pleural cavities, B-1 cells were depleted from both cavities (52). We adapted a protocol described by Murakami and Honjo (53), wherein

hypotonic shock results in selective depletion of self-replenishing B-1 cells in the peritoneal cavity, but not in the spleen (54, 55). Briefly, 2–4 week old C57BL/6 mice were injected *i.p.* and *i.t.* with 0.5 ml and 0.1 ml of ddH_20, respectively, every week until infection. At 4–8 weeks, mice received 1 ml and 0.2 ml of ddH_20 *i.p.* and *i.t.*, respectively. Control groups were injected with PBS at all times. Depletion was performed for three weeks before CN infection. Selective depletion of B-1 cells was confirmed by flow-cytometry. The groups of B-1 depleted and control mice were infected *i.n.* with 5×10^5 CFU of CN strain 24067 and euthanized on day 3 post-infection.

B-1a cell transfer

Total PerC cells from 6–8 weeks old C57BL/6 mice were isolated and stained with CD45-Pacific Blue, CD19-PE-Cy7, B220-PerCP-Cy5.5, IgD-APC, CD5-PE, and IgM-FITC (BD Biosciences). B-1a cells ($CD45^+CD19^{hi}B220^{int}IgD^{int}IgM^{hi}CD5^+$) were bulk sorted and transferred *i.p.* to B-1 depleted mice (5×10^5 cells per mouse) 24 hrs prior to *i.n.* infection with 5×10^5 CFU of strain 24067. Mice were euthanized on day 3 post-infection.

Phagocytosis Analysis and Fungal Burden

Alveolar macrophages were isolated from the lung lavage fluid of mice euthanized on day 3 post-infection as described previously (27). Macrophages were allowed to attach on slide chambers for 2 hrs, fixed with methanol and stained with Geimsa. Cells were examined under 40X magnification. The phagocytic index (PI) was defined as number of internalized CN cells per 100 macrophages counted. After collecting the lung lavages, lungs and brains were removed and homogenized in 1 ml of HBSS (Lonza). CFUs were determined by making 10-fold serial dilutions of each tissue and plating 20 μl of the dilutions on Sabouraud Dextrose agar plates, in duplicate. Plates were incubated at room temperature for 72 hours, after which colonies were visually counted.

Statistical Analysis

All statistical analyses were performed using Prism (Graphpad). For comparison between two groups, Student t test was used. Multigroup comparisons of mean values were made using one-way ANOVA followed by Bonferroni's post-test. Gene family usage and N nucleotide additions were compared using the χ^2 test as described (56). All combinations were compared in 2×2 contingency tables. For statistical evaluations, $p<0.05$ was considered significant.

Results

The early B cell response to CN is most robust in PerC B-1 B cells

Total B, B-2, B-1a and B-1b B cells in lungs, medLN, spleen and PerC of naïve and day 7 CN-infected C57BL/6 mice were quantified to identify sites of the early B cell response to CN. There was an increase of total lymphocytes in medLN on day 7 post-infection, which was mainly limited to the B-2 subpopulation (Fig 1A). Total B-1a, B-1b and B-2 cell numbers increased in lungs on day 7, but were comparable in spleen and PerC of CN-infected and naïve mice (Fig 1B, 1C and 1D). We next analyzed earlier times and found a significant increase in total PerC B-1a, B-1b and B-2 cells on day 1 post-infection that peaked on day 3 post-infection (Fig 1C). Differences in lung B-1a, B-1b and B-2 cells in infected and control mice on day 1 were not statistically significant (Fig 1D) and the increase in lung total B, B-2 and B-1 cells seen on day 3, did not reach statistical significance for B-1a cells (Fig 1D).

ELISPOTS were used to determine if CN-infection induced B cells observed in PerC, spleen, medLN and lungs, produced IgM that bound to GXM- and heat-killed capsular

(24067) and acapsular (Cap67) CN. On day 3 post-infection, PerC and splenic B cells were the main source of CN-binding IgM (Fig 1E). As PerC B cells were increased by day 1 post-infection and were the main source of CN-binding IgM, subsequent analyses were performed on PerC cells.

The early B cell response to CN is due to recruitment

We examined the rate of BrdU incorporation on day 3 post-infection to establish whether the increase in PerC B cells in CN-infected mice was due to migration and recruitment of B cells or clonal expansion. BrdU incorporation was not significantly different in naïve (sham-infected) and infected mice (1.7% vs. 2.5% for Total B, 0.57% vs. 0.89% for B-2, 3% vs. 5% for B-1a, and 1.8% vs. 2.6% for B-1b cells). Hence, the increase in B cells reflected recruitment.

PerC B-1a B cells have the highest frequency of CN-binding cells

To investigate whether the B cells recruited to PerC in CN-infected mice were selected due to an intrinsic capacity for CN binding, we used GFP labeled capsular 24067 (GFP-24067) and Uvitex labeled acapsular Cap67 (Uvitex-Cap67) strains to select, respectively, capsular and acapsular CN-binding B-1a, B-1b and B-2 cells by flow cytometry (Fig 2). Both strains were used to identify differences in the frequency of B-1a, B-1b and B-2 B cells that bind capsular and acapsular (cell wall) antigens. Compared to naïve mice, on day 3 post-infection, PerC acapsular CN-binding B-1a, B-1b and B-2 cells increased from 0.05% to 0.30%, 0.03% to 0.17% and 0.06% to 0.25%, respectively (Fig 2A). Although the frequency of both capsular and acapsular CN-selected cells was higher in each B cell population among CN-infected than naïve mice, B-1a B cells exhibited the most capsular (5% vs. 2%, $p=0.02$) (Fig 2B) and acapsular (18% vs. 11%, $p=0.07$) (Fig 2C) CN binding. Differences in CN-selected cells in B-1b and B-2 populations did not reach significance. On day 7 post-infection, the frequency of B cell subsets in CN-infected mice was similar to that of naïve mice (data not shown).

ELISPOT to determine specificity of CN-binding B cells

Acapsular (Uvitex-Cap67) CN-selected B cells that were obtained by FACS were assayed for IgM binding to laminarin (a β-1,3-glucan present on fungal cell walls), purified GXM, and heat-killed 24067 and Cap67 CN cells by ELISPOT. Capsular (GFP-24067) CN-selected cells were not present in a high enough frequency to analyze. Unselected and CN-selected cells identified by Uvitex-Cap67 binding had a similar frequency of IgM-producing cells (data not shown). However, compared to unselected cells, Uvitex-Cap67-binding B cells had a 2–5 fold higher frequency of laminarin binding B-1 and B-2 cells ($p<0.05$) (Fig 2D). CN-selected cells also showed increased binding to GXM and heat-killed 24067 and Cap67 CN cells, compared to unselected cells (not shown). Hence, CN-selected cells produced IgM that bound to CN antigens.

B-1a cells that bind acapsular and capsular CN express V_H11 and $V_H12$genes

V_H gene use of CN-selected B cells was analyzed because V_H genes are a determinant of antigen binding and a bias, or restriction, in gene use could link susceptibility to CN to the loss of CN-binding B cells. The molecular repertoire of CN-selected PerC B cells was determined 3 days after CN infection by immunoglobulin gene sequence analysis of unselected, acapsular (Uvitex-Cap67$^+$)-, and capsular (GFP-24067$^+$) CN-selected B-1a, B-1b and B-2 cells. A total of 182 single cells were sequenced from two independent cell-sortings, which included 51 B-2, 68 B-1a, and 63 B-1b sequences (Supplemental Table I).

Figure 3 shows IgV_H gene family frequencies in unselected-, acapsular- and capsular-CN-selected B-1a, B-1b and B-2 cells. J558 (V_H1) usage predominated in unselected B-2 (40%; Fig 3A), B-1a (33.3%; Fig 3B) and B-1b cells (41%; Fig 3C) with frequencies similar to expected germline frequencies (56). Acapsular CN-selected B-2 cells had evidence of antigen-driven selection, with a significantly higher frequency of J558 genes (83%, Fig 3D) than unselected (40%, p=0.02, Fig 3A) and capsular CN-selected B-2 cells (27%, p=0.02, Fig 3G). Capsular CN-selected B-2 B cells had a higher frequency of Q52 (18% vs. 0), 7183 (9% vs. 7%) and S107 (18% vs. 7%) gene use than unselected B-2 cells (Fig 3G).

For B-1a cells, J558 gene use was similar in unselected- (33%, Fig 3B), acapsular- (22%, Fig 3E) and capsular- (20%, Fig 3H) CN-selected cells. However, acapsular CN-selected B-1a cells had more V_H11 gene use (22%, Fig 3E) than unselected cells (11%, Fig 3B), and capsular CN-selected B-1a cells had 10 times more V_H12 gene use (33%, Fig 3H) than unselected cells (3%, p=0.02, Fig 3B). Although all acapsular (V_H11^+) and capsular (V_H12^+) CN-selected B-1a cells used the same VH11.2.53 and VH12.1.78 genes, respectively, most were independent rearrangements (Supplemental Table I). Sixty percent of V_H11^+ B-1a cells and 80% of V_H12^+ B-1a cells had different D_H segments paired with J_H1. The number of sequences obtained limited further conclusions about the other genes used by B-1a cells.

For B-1b cells, V_H gene use was similar to previous reports (56). J558 gene use was similar in unselected (41%, Fig 3C), acapsular (40%, Fig 3F) and capsular (36%, Fig 3I) CN-selected cells. There were no differences in the use of other gene families among CN-selected and unselected B-1b cells.

There were no differences in D_H or J_H gene use in unselected and CN-selected B-1a, B-1b and B-2 cells (Supplemental Fig 1 and Fig 2) and patterns of use were similar to previous reports (56, 57). The majority of B cells analyzed utilized the DSP and DFL16 family D_H gene segments. Increased J_H1 usage (60%) observed in GFP-24067$^+$ B-1a cells was due to preferential pairing of V_H11 and V_H12 genes with J_H1.

B cells that bind acapsular and capsular CN differ in their clan derivation

As it has been hypothesized that clans of structurally related immunoglobulins bind defined antigenic determinants (58), we classified the V_H gene family usage of the B cell subsets described above into these clans (Fig 4). Compared to unselected cells, there was increased clan 1/J558 usage in acapsular CN-selected B-2 cells (92% vs. 75%, Fig 4D and Fig 4A) and B-1b cells (55% vs. 45%, Fig 4F and 4C). In contrast, increased clan II gene use was seen in capsular CN-selected B-2 (18% vs. 11%, Fig 4G and Fig 4A), B-1a (47% vs. 23%, Fig 4H and Fig 4B), and B-1b (28% vs. 17%, Fig 4I and 4C) cells compared to unselected counterparts. Increased clan III usage in acapsular CN-selected B-1a cells did not reach statistical significance (39% vs. 30%, Fig 4E and Fig 4B).

HCDR3 regions of CN-selected and unselected B-1a cells vary in Glycine content and length

Since PerC B-1a cells had the most CN-selected cells among the B-cell populations analyzed, we examined their HCDR sequences to gain further insight into their role in CN binding (Supplemental Table II). All 68 B-1a B-cell sequences were essentially germline. Compared to unselected cells, CN-selected B-1a cells had a significantly higher frequency of Glycine residues (11% vs. 6%, p=0.03). HCDR2 sequences were analyzed to detect residues 51/I, 54/G, 58/Y, 59/Y, 61/D and 63/V, which were conserved in human and mouse GXM-binding mAbs (17, 59). Residues 51/I and 59/Y were conserved in 95% and 100%, respectively, of all 68 B-1a sequences. 54/G was conserved in both acapsular (48%) and

capsular (53%) CN-selected B-1a cells compared to unselected (36%) B-1a sequences. No significant conservation was observed for 58/Y, 61/D and 63/V or HCDR3 residues 95/R and 96/D. Consistent with other reports (56, 57), HCDR3 lengths of B-1a (Av. 10.8 ± 2.6 codons) were shorter than those of B-2 and B-1b cells. HCDR3 lengths of 11 amino acids were more frequent in acapsular CN-selected B-1a (26% vs. 13%) than unselected cells, and lengths of 12 amino acids were more frequent in capsular CN-selected B-1a (33% vs. 16%) than unselected cells (Fig. 5A).

N-nucleotide additions differ in acapsular- and capsular- CN-binding B-1a subsets

N nucleotides increase HCDR3 length and generate junctional diversity (60). In our analysis, shorter HCDR3 lengths in B-1a cells were associated with fewer N-additions. Sequences having ≤ 3 N-additions were considered close to germline. More B-1a cells (56%) had ≤ 3 N-additions than B-2 (22%, $p<0.01$) and B-1b (35%, $p=0.02$) cells and there were fewer N-additions in acapsular and capsular CN-selected B-1a cells (Av. 2.5 vs. 4.0) than unselected B-1a cells. The majority (57%) of unselected B-1a cells had > 3 N-nucleotides, compared to 40% of acapsular- and only 26% of capsular CN-selected B-1a cells (Fig 5B); demonstrating that capsular CN-selected B-1a cells were significantly more germline than unselected ($p<0.05$) and acapsular CN-selected B-1a cells, although the latter difference was not statistically significant.

Depletion of B-1 cells results in increased fungal burden and reduced phagocytosis

To establish a mechanistic role for B-1a cells in our model, we depleted mice of pleural and PerC B-1 cells and compared fungal burdens and alveolar macrophage phagocytosis of CN in depleted and un-depleted (control) mice. After 3 weeks of depletion, B-1 cell numbers were lower in B-1 depleted mice (30%) than un-depleted mice by flow-cytometry (Fig 6A and B). B-1 depleted mice had more CFUs in lung ($p=0.002$) and brain ($p=0.01$) three days after CN infection (Fig 6C and D). As *in vivo* phagocytosis is a correlate of survival in pulmonary CN infection models (27, 61), we also determined *in vivo* phagocytosis, *ex vivo*. Alveolar macrophages from control mice had a significantly higher phagocytic index (PI) than B-1 depleted ($p=0.04$) mice (Fig 6E). Next, we reconstituted B-1 B cell depleted mice with B-1a B cells and evaluated the same parameters. Lung ($p=0.005$) and brain ($p=0.03$) CFUs were lower in B-1a B cell reconstituted than B-1 B cell depleted mice and B-1a B cell reconstituted mice had significantly more alveolar phagocytosis than B-1 depleted mice ($p=0.02$) (Fig 6H).

Discussion

Our data provide direct evidence that B-1a cells contribute to early clearance of CN in a pulmonary infection model. B-1 B-cell depleted CN-infected mice had higher fungal burdens and less robust alveolar macrophage phagocytosis of CN than control and B-1a reconstituted B-1 B-cell depleted mice. Hence, as described for other pathogens (22, 45, 62), B-1a B cells also provide a first line of defense against pulmonary CN infection in mice. Cells from PerC and spleen showed increased IgM production in response to CN infection. As CN-infected mice exhibited an early increase in IgM-secreting PerC B-1 B cells and a previous study demonstrated that natural IgM enhanced alveolar macrophage phagocytosis of CN in IgM deficient mice (27), our findings suggest that B-1a B cells enhance innate anti-fungal immunity via natural IgM. Consistent with murine influenza virus studies (23, 62–64), the increases in PerC and lung B-1 B cells in our model were due to recruitment, rather than clonal expansion. Although the mechanism by which B-1 B cells traffic to CN-infected lungs requires additional study, PerC B-1 cells migrate in response to chemokines, can differentiate into phagocytes that move to inflammatory loci (65–68) and have been shown to kill CN *in vitro* (40).

B-1 B cell-derived IgM bound to acapsular and capsular CN cells, GXM, and laminarin. However, it is likely that laminarin, a β 1–3 glucan that is part of the CN cell wall (13) was a main capsular and acapsular CN IgM binding determinant. MAbs to laminarin bound to *Candida albicans*, *Aspergillus fumigatus* and CN and protected mice from lethal *Candida* and CN infection (13, 14, 29, 69). We were not able to discriminate between B-1a- and B-1b-derived CN-binding IgM due to the limited number of B-1a and B-1b cells recovered. In other mouse models, $CD5^+$ (B-1a) B cells produced laminarin-reactive IgM after *Pneumocystis* infection (22) and B-1a cells mediated protection against *Francisella tularensis* (45), but B-1b cells protected against *Borrelia hermsii* (70, 71) and B-1a and B-1b cells had different roles in resistance to *Streptococcus pneumoniae.* For the latter, B-1a cells mediated protection via natural antibodies to phosphorylcholine (PC) and B-1b cells generated capsular polysaccharide antibodies (35). It is possible that B-1b cells were also responsible for capsular polysaccharide (GXM) reactivity in our model, but technical challenges prevented us from isolating GXM^+ B cells.

Sequence analysis of CN-binding B-1a B cells revealed V_H restriction, albeit to different V_H genes than those used in GXM mAbs (16). Interestingly, the gene element (V_H7183) used in the GXM-elicited repertoire was only slightly increased in capsular CN-selected B-2 cells, suggesting that GXM determinants that are targets of the adaptive response are not a predominant focus of the early innate B-cell response. We were not able to study GXM-selected B cells. Alternatively, the minimal increase in CN-selected B cells expressing V_H genes used in GXM mAbs could indicate that capsular polysaccharide determinants are recognized differently in the context of whole organism as described for another encapsulated pathogen (72, 73). Although the biological significance of V_H restriction is not known, many restricted responses are focused on conserved microbial determinants, such as α (1–3) dextran (J558/V_H1); phosphorylcholine, PC (T15/V_H7), and phosphatidylcholine, PtC (V_H11 and V_H12) (74). Strikingly, acapsular CN-selected B-1a B cells used V_H11, whereas capsular CN-selected cells used V_H12 genes. V_H11 and V_H12 gene segments each confer specificity for PtC (74, 75) and B-1a cells produce natural antibodies to PtC (76), a mammalian and bacterial membrane phospholipid that has also been discovered in CN vesicles (77). As the restricted repertoire of PtC-reactive B-1 cells and their predominant pairing with J_H1 is thought to enable B-1 cells to respond to microbial antigens (78), PtC–rich CN vesicles could shape the early B cell response to CN.

Although V_H11 and V_H12 gene segments are both implicated in PtC binding, they belong to different immunoglobulin clans (58), with V_H11 belonging to clan III and V_H12 belonging to clan II. The difference in V_H gene usage that we observed among acapsular (V_H11) and capsular (V_H12) CN-selected B-1a cells suggests that different PtC-like determinants are recognized in each case and/or that PtC is recognized differently in the context of capsular polysaccharide. The latter has been demonstrated for the response to pneumococcal proteins (79). However, we note that GFP-24067 (capsular CN) could have captured B cells recognizing capsular as well as cell wall components. Our data indicate that glucans present on the CN cell wall (80) also shape the early CN response as reflected by laminarin (β-glucan) binding of CN-selected B-1 B cells. Further, and in contrast to capsular CN-selected B-1 cells, acapsular CN-selected B-1b and B2 cells exhibited predominant use of clan 1/ V_HJ558. As natural antibodies to α 1–3 dextran use clan I/J558 gene segments (81, 82) and α 1–3 glucans are present on the CN cell wall (83, 84), our data suggest that acapsular CN-selected B-2 and B-1b cells bind antigens that are discrete from those recognized by B-1a B cells.

HCDR3 regions, which are critical for antigen recognition (85), are biased to the use of neutral, hydrophilic amino acids such as Tyrosine, Glycine and Serine, and against the use of highly charged and hydrophobic amino acids (86, 87). Our data show that Glycine use

was much higher in CN-selected than unselected cells corroborating previous data that carbohydrate-binding CDR3s preferentially use hydrophilic amino acids (51). Consistent with studies showing that HCDR2 residues are also critical for the generation of human and mouse antibodies to GXM (17, 59), we found that the HCDR2 residues I/51, G/54, and Y/59 were conserved in CN-binding B-1a cells. Thus, our data support the concept that V_H as well as HCDR2 and HCDR3, each confer binding to CN determinants (88). Further, as restriction in HCDR3 length is indicative of antigen-driven selection, our finding that capsular CN-selected cells had shorter HCDR3 lengths than acapsular CN-selected cells, provides further evidence that capsular and acapsular CN select distinct germline B cell repertoires.

There was no evidence of somatic hypermutation in any of the B-1a cells we studied. As human GXM-binding mAbs derived from XenoMouse mice also used germline V_H gene segments (17), our data further demonstrate that restricted V_H genes and conserved HCDR structures are sufficient to bind CN determinants. Our data also confirm reports that B-1a cells have a low frequency of N-nucleotides (56, 57) and reveal that acapsular CN-selected B-1a cells had more N-nucleotides than capsular CN-selected cells. Thus, TdT activity could be more important for binding to β-glucan and/or other CN cell wall determinants than GXM. Consistent with the latter, TdT was required for optimal antibody responses to the α-glucan dextran (89). As noted above, the molecular features of acapsular and capsular CN-binding B-1a cells differed from those observed for GXM-binding mAbs generated from GXM-TT vaccinated mice, which mainly used 7183 V_H, a member of clan III (15, 16, 90). Similarly, human mAbs elicited by a GXM conjugate (in XenoMouse mice), used V_H3 and V_H6, members of clans III and clan II, respectively (17). In our study, the increase in clan III use only reached statistical significance for CN-selected B-2 cells. Hence, the molecular features of ‘innate’ and ‘adaptive’ responses to CN differ. The ‘adaptive’ response, as exemplified by GXM-binding mAbs, is derived from Clan III genes, whereas the ‘innate’ response, as reported herein, is dominated by B-1a cells expressing germline Clan I and II genes. As the ‘innate’ response is likely to be stimulated by cell wall carbohydrate (glucans) and/or phosphorylated determinants (e.g. PtC), our data are consistent with reports that the primary and secondary responses of B-1a cells are distinct from B-2 cells (91, 92).

To our knowledge, this study is the first to establish a role for the germline B-1 repertoire in the innate response to CN as our data show that B-1a B cells contribute to fungal clearance and enhance phagocytosis of CN in the lungs. Given that IgM memory B cells are a major source of natural IgM (21, 38), our findings provide a potential explanation for the observation that loss of IgM memory B cells was associated with risk for HIV-associated cryptococcosis (24). More work is needed to discriminate between the contributions of B-1a B cells and IgM in host defense against CN and to identify the precise CN determinants that B-1a B cells recognize. Nonetheless, our discovery that the naturally occurring B cell repertoire has the ability to respond to CN has broad implications for our understanding of the pathogenesis of CN and advancing new approaches to treat and prevent cryptococcosis.

Supplementary Material

Refer to Web version on PubMed Central for supplementary material.

Acknowledgments

We thank the AECOM Flow Cytometry Core Facility under the support of the AECOM National Cancer Institute (P30CA013330) for assistance with data acquisition.

This work was supported by NIH grant R01-AI097096 to LP.

Abbreviations used in this paper

CN	*Cryptococcus neoformans*
PerC	peritoneal cavity
medLN	mediastinal lymph nodes
GXM	glucuronoxylomannan
vs	versus
N	nontemplate encoded
P	palindromic
PtC	phosphatidyl choline
PC	phosphorylcholine

References

1. Huffnagle GB, Lipscomb MF, Lovchik JA, Hoag KA, Street NE. The role of CD4+ and CD8+ T cells in the protective inflammatory response to a pulmonary cryptococcal infection. Journal of Leukocyte Biology. 1994; 55:35–42. [PubMed: 7904293]
2. Huffnagle GB, Yates JL, Lipscomb MF. Immunity to a pulmonary Cryptococcus neoformans infection requires both CD4+ and CD8+ T cells. J Exp Med. 1991; 173:793–800. [PubMed: 1672543]
3. Dromer F, Salamero J, Contrepois A, Carbon C, Yeni P. Production, characterization, and antibody specificity of a mouse monoclonal antibody reactive with Cryptococcus neoformans capsular polysaccharide. Infection and Immunity. 1987; 55:742–8. [PubMed: 3546139]
4. Eckert TF, Kozel TR. Production and characterization of monoclonal antibodies specific for Cryptococcus neoformans capsular polysaccharide. Infection and Immunity. 1987; 55:1895–9. [PubMed: 2440810]
5. Mukherjee S, Lee SC, Casadevall A. Antibodies to Cryptococcus neoformans glucuronoxylomannan enhance antifungal activity of murine macrophages. Infection and Immunity. 1995; 63:573–9. [PubMed: 7822024]
6. Casadevall A, Cleare W, Feldmesser M, Glatman-Freedman A, Goldman DL, Kozel TR, Lendvai N, Mukherjee J, Pirofski LA, Rivera J, Rosas AL, Scharff MD, Valadon P, Westin K, Zhong Z. Characterization of a murine monoclonal antibody to Cryptococcus neoformans polysaccharide that is a candidate for human therapeutic studies. Antimicrobial Agents and Chemotherapy. 1998; 42:1437–46. [PubMed: 9624491]
7. Fleuridor R, Lees A, Pirofski L. A cryptococcal capsular polysaccharide mimotope prolongs the survival of mice with Cryptococcus neoformans infection. Journal of Immunology (Baltimore, Md : 1950). 2001; 166:1087–96.
8. Dromer F, Charreire J, Contrepois A, Carbon C, Yeni P. Protection of mice against experimental cryptococcosis by anti-Cryptococcus neoformans monoclonal antibody. Infect Immun. 1987; 55:749–752. [PubMed: 3546140]
9. Schlageter AM, Kozel TR. Opsonization of Cryptococcus neoformans by a family of isotype-switch variant antibodies specific for the capsular polysaccharide. Infect Immun. 1990; 58:1914–1918. [PubMed: 2187813]
10. Shapiro S, Beenhouwer DO, Feldmesser M, Taborda C, Carroll MC, Casadevall A, Scharff MD. Immunoglobulin G monoclonal antibodies to Cryptococcus neoformans protect mice deficient in complement component C3. Infect Immun. 2002; 70:2598–2604. [PubMed: 11953401]
11. Miller MF, Mitchell TG, Storkus WJ, Dawson JR. Human natural killer cells do not inhibit growth of Cryptococcus neoformans in the absence of antibody. Infect Immun. 1990; 58:639–645. [PubMed: 2407651]

12. Nabavi N, Murphy JW. Antibody-dependent natural killer cell-mediated growth inhibition of Cryptococcus neoformans. Infect Immun. 1986; 51:556–562. [PubMed: 3510982]
13. Torosantucci A, Chiani P, Bromuro C, De Bernardis F, Palma AS, Liu Y, Mignogna G, Maras B, Colone M, Stringaro A, Zamboni S, Feizi T, Cassone A. Protection by anti-beta-glucan antibodies is associated with restricted beta-1,3 glucan binding specificity and inhibition of fungal growth and adherence. PloS One. 2009; 4:e5392. [PubMed: 19399183]
14. Torosantucci A, Bromuro C, Chiani P, De Bernardis F, Berti F, Galli C, Norelli F, Bellucci C, Polonelli L, Costantino P, Rappuoli R, Cassone A. A novel glyco-conjugate vaccine against fungal pathogens. J Exp Med. 2005; 202:597–606. [PubMed: 16147975]
15. Mukherjee J, Casadevall A, Scharff MD. Molecular characterization of the humoral responses to Cryptococcus neoformans infection and glucuronoxylomannan-tetanus toxoid conjugate immunization. The Journal of Experimental Medicine. 1993; 177:1105–16. [PubMed: 8459205]
16. Casadevall A, DeShaw M, Fan M, Dromer F, Kozel TR, Pirofski LA. Molecular and idiotypic analysis of antibodies to Cryptococcus neoformans glucuronoxylomannan. Infection and Immunity. 1994; 62:3864–72. [PubMed: 8063403]
17. Maitta RW, Datta K, Chang Q, Luo RX, Witover B, Subramaniam K, Pirofski LA. Protective and nonprotective human immunoglobulin M monoclonal antibodies to Cryptococcus neoformans glucuronoxylomannan manifest different specificities and gene use profiles. Infection and Immunity. 2004; 72:4810–8. [PubMed: 15271943]
18. Maitta RW, Datta K, Lees A, Belouski SS, Pirofski LA. Immunogenicity and efficacy of Cryptococcus neoformans capsular polysaccharide glucuronoxylomannan peptide mimotope-protein conjugates in human immunoglobulin transgenic mice. Infect Immun. 2004; 72:196–208. [PubMed: 14688097]
19. Pirofski LA. Polysaccharides, mimotopes and vaccines for fungal and encapsulated pathogens. Trends Microbiol. 2001; 9:445–451. [PubMed: 11553457]
20. Moir S, Fauci AS. B cells in HIV infection and disease. Nat Rev Immunol. 2009; 9:235–245. [PubMed: 19319142]
21. Carsetti R, Rosado MM, Donnanno S, Guazzi V, Soresina A, Meini A, Plebani A, Aiuti F, Quinti I. The loss of IgM memory B cells correlates with clinical disease in common variable immunodeficiency. J Allergy Clin Immunol. 2005; 115:412–417. [PubMed: 15696104]
22. Rapaka RR, Ricks DM, Alcorn JF, Chen K, Khader SA, Zheng M, Plevy S, Bengten E, Kolls JK. Conserved natural IgM antibodies mediate innate and adaptive immunity against the opportunistic fungus Pneumocystis murina. The Journal of Experimental Medicine. 2010; 207:2907–19. [PubMed: 21149550]
23. Baumgarth N. The double life of a B-1 cell: self-reactivity selects for protective effector functions. Nature Reviews Immunology. 2011; 11:34–46.
24. Subramaniam K, Metzger B, Hanau LH, Guh A, Rucker L, Badri S, Pirofski LA. IgM(+) memory B cell expression predicts HIV-associated cryptococcosis status. The Journal of Infectious Diseases. 2009; 200:244–51. [PubMed: 19527168]
25. Fleuridor R, Lyles RH, Pirofski L. Quantitative and qualitative differences in the serum antibody profiles of human immunodeficiency virus-infected persons with and without Cryptococcus neoformans meningitis. J Infect Dis. 1999; 180:1526–1535. [PubMed: 10515812]
26. Pirofski L, Lui R, DeShaw M, Kressel AB, Zhong Z. Analysis of human monoclonal antibodies elicited by vaccination with a Cryptococcus neoformans glucuronoxylomannan capsular polysaccharide vaccine. Infection and Immunity. 1995; 63:3005–14. [PubMed: 7622223]
27. Subramaniam KS, Datta K, Quintero E, Manix C, Marks MS, Pirofski LA. The absence of serum IgM enhances the susceptibility of mice to pulmonary challenge with Cryptococcus neoformans. Journal of Immunology (Baltimore, Md : 1950). 2010; 184:5755–67.
28. Li W, Fu M, An JG, Xing Y, Zhang P, Zhang X, Wang YC, Li CX, Tian R, Su WJ, Guan HH, Wang G, Gao TW, Han H, Liu YF. Host defence against C. albicans infections in IgH transgenic mice with V(H) derived from a natural anti-keratin antibody. Cell Microbiol. 2007; 9:306–315. [PubMed: 16925788]
29. Rachini A, Pietrella D, Lupo P, Torosantucci A, Chiani P, Bromuro C, Proietti C, Bistoni F, Cassone A, Vecchiarelli A. An anti-beta-glucan monoclonal antibody inhibits growth and capsule

formation of Cryptococcus neoformans in vitro and exerts therapeutic, anticryptococcal activity in vivo. Infect Immun. 2007; 75:5085–5094. [PubMed: 17606600]

30. Monga DP, Kumar R, Mohapatra LN, Malaviya AN. Experimental cryptococcosis in normal and B-cell-deficient mice. Infect Immun. 1979; 26:1–3. [PubMed: 387600]
31. Aguirre KM, Johnson LL. A role for B cells in resistance to Cryptococcus neoformans in mice. Infect Immun. 1997; 65:525–530. [PubMed: 9009308]
32. Feldmesser M, Mednick A, Casadevall A. Antibody-mediated protection in murine Cryptococcus neoformans infection is associated with pleotrophic effects on cytokine and leukocyte responses. Infect Immun. 2002; 70:1571–1580. [PubMed: 11854246]
33. Rivera J, Zaragoza O, Casadevall A. Antibody-mediated protection against Cryptococcus neoformans pulmonary infection is dependent on B cells. Infect Immun. 2005; 73:1141–1150. [PubMed: 15664957]
34. Marquis G, Montplaisir S, Pelletier M, Mousseau S, Auger P. Genetic resistance to murine cryptococcosis: increased susceptibility in the CBA/N XID mutant strain of mice. Infect Immun. 1985; 47:282–287. [PubMed: 3880724]
35. Haas KM, Poe JC, Steeber DA, Tedder TF. B-1a and B-1b cells exhibit distinct developmental requirements and have unique functional roles in innate and adaptive immunity to S. pneumoniae. Immunity. 2005; 23:7–18. [PubMed: 16039575]
36. Hardy RR. B-1 B cell development. J Immunol. 2006; 177:2749–2754. [PubMed: 16920907]
37. Ghosn EE, Yamamoto R, Hamanaka S, Yang Y, Herzenberg LA, Nakauchi H, Herzenberg LA. Distinct B-cell lineage commitment distinguishes adult bone marrow hematopoietic stem cells. Proc Natl Acad Sci U S A. 2012; 109:5394–5398. [PubMed: 22431624]
38. Carsetti R, Rosado MM, Wardmann H. Peripheral development of B cells in mouse and man. Immunol Rev. 2004; 197:179–191. [PubMed: 14962195]
39. Almeida SR, Aroeira LS, Frymuller E, Dias MA, Bogsan CS, Lopes JD, Mariano M. Mouse B-1 cell-derived mononuclear phagocyte, a novel cellular component of acute non-specific inflammatory exudate. Int Immunol. 2001; 13:1193–1201. [PubMed: 11526100]
40. Ghosn EE, Russo M, Almeida SR. Nitric oxide-dependent killing of Cryptococcus neoformans by B-1-derived mononuclear phagocyte. Journal of Leukocyte Biology. 2006; 80:36–44. [PubMed: 16670124]
41. Ghosh S, Hoselton SA, Schuh JM. mu-chain-deficient mice possess B-1 cells and produce IgG and IgE, but Not IgA, following systemic sensitization and inhalational challenge in a fungal asthma model. J Immunol. 2012; 189:1322–1329. [PubMed: 22732592]
42. Subramaniam KS, Datta K, Marks MS, Pirofski LA. Improved survival of mice deficient in secretory immunoglobulin M following systemic infection with Cryptococcus neoformans. Infection and Immunity. 2010; 78:441–52. [PubMed: 19901068]
43. Mukherjee J, Scharff MD, Casadevall A. Protective murine monoclonal antibodies to Cryptococcus neoformans. Infection and Immunity. 1992; 60:4534–41. [PubMed: 1398966]
44. Szymczak WA, Sellers RS, Pirofski LA. IL-23 Dampens the Allergic Response to Cryptococcus neoformans through IL-17-Independent and -Dependent Mechanisms. The American Journal of Pathology. 2012; 180:1547–59. [PubMed: 22342846]
45. Cole LE, Yang Y, Elkins KL, Fernandez ET, Qureshi N, Shlomchik MJ, Herzenberg LA, Herzenberg LA, Vogel SN. Antigen-specific B-1a antibodies induced by Francisella tularensis LPS provide long-term protection against F. tularensis LVS challenge. Proceedings of the National Academy of Sciences of the United States of America. 2009; 106:4343–8. [PubMed: 19251656]
46. Newman J, Rice JS, Wang C, Harris SL, Diamond B. Identification of an antigen-specific B cell population. Journal of Immunological Methods. 2003; 272:177–87. [PubMed: 12505722]
47. Nimrichter L, Frases S, Cinelli LP, Viana NB, Nakouzi A, Travassos LR, Casadevall A, Rodrigues ML. Self-aggregation of Cryptococcus neoformans capsular glucuronoxylomannan is dependent on divalent cations. Eukaryotic Cell. 2007; 6:1400–10. [PubMed: 17573547]
48. Tiller T, Busse CE, Wardemann H. Cloning and expression of murine Ig genes from single B cells. Journal of Immunological Methods. 2009; 350:183–93. [PubMed: 19716372]

49. Kantor AB, Merrill CE, MacKenzie JD, Herzenberg LA, Hillson JL. Development of the antibody repertoire as revealed by single-cell PCR of FACS-sorted B-cell subsets. Annals of the New York Academy of Sciences. 1995; 764:224–7. [PubMed: 7486528]
50. Rohatgi S, Ganju P, Sehgal D. Systematic design and testing of nested (RT−)PCR primers for specific amplification of mouse rearranged/expressed immunoglobulin variable region genes from small number of B cells. Journal of Immunological Methods. 2008; 339:205–19. [PubMed: 18926828]
51. Rohatgi S, Dutta D, Tahir S, Sehgal D. Molecular dissection of antibody responses against pneumococcal surface protein A: evidence for diverse DH-less heavy chain gene usage and avidity maturation. Journal of Immunology (Baltimore, Md : 1950). 2009; 182:5570–85.
52. Bogsan CS, Novaes e Brito RR, Palos C, da M, Mortara RA, Almeida SR, Lopes JD, Mariano M. B-1 cells are pivotal for in vivo inflammatory giant cell formation. Int J Exp Pathol. 2005; 86:257–265. [PubMed: 16045548]
53. Murakami M, Yoshioka H, Shirai T, Tsubata T, Honjo T. Prevention of autoimmune symptoms in autoimmune-prone mice by elimination of B-1 cells. Int Immunol. 1995; 7:877–882. [PubMed: 7547714]
54. Peterson LK, Tsunoda I, Fujinami RS. Role of CD5+ B-1 cells in EAE pathogenesis. Autoimmunity. 2008; 41:353–362. [PubMed: 18568640]
55. Renner B, Strassheim D, Amura CR, Kulik L, Ljubanovic D, Glogowska MJ, Takahashi K, Carroll MC, Holers VM, Thurman JM. B cell subsets contribute to renal injury and renal protection after ischemia/reperfusion. J Immunol. 2010; 185:4393–4400. [PubMed: 20810984]
56. Kantor AB, Merrill CE, Herzenberg LA, Hillson JL. An unbiased analysis of V(H)-D-J(H) sequences from B-1a, B-1b, and conventional B cells. Journal of Immunology (Baltimore, Md : 1950). 1997; 158:1175–86.
57. Tornberg UC, Holmberg D. B-1a, B-1b and B-2 B cells display unique VHDJH repertoires formed at different stages of ontogeny and under different selection pressures. The EMBO Journal. 1995; 14:1680–9. [PubMed: 7737121]
58. Kirkham PM, Mortari F, Newton JA, SHW. Immunoglobulin VH clan and family identity predicts variable domain structure and may influence antigen binding. The EMBO Journal. 1992; 11:603–9. [PubMed: 1537339]
59. Nakouzi A, Casadevall A. The function of conserved amino acids in or near the complementarity determining regions for related antibodies to Cryptococcus neoformans glucuronoxylomannan. Molecular Immunology. 2003; 40:351–61. [PubMed: 14522016]
60. Shiokawa S, Mortari F, Lima JO, Nunez C, Bertrand FE 3rd, Kirkham PM, Zhu S, Dasanayake AP, Schroeder HW Jr. IgM heavy chain complementarity-determining region 3 diversity is constrained by genetic and somatic mechanisms until two months after birth. J Immunol. 1999; 162:6060–6070. [PubMed: 10229847]
61. Zaragoza O, Alvarez M, Telzak A, Rivera J, Casadevall A. The relative susceptibility of mouse strains to pulmonary Cryptococcus neoformans infection is associated with pleiotropic differences in the immune response. Infect Immun. 2007; 75:2729–2739. [PubMed: 17371865]
62. Choi YS, Baumgarth N. Dual role for B-1a cells in immunity to influenza virus infection. The Journal of Experimental Medicine. 2008; 205:3053–64. [PubMed: 19075288]
63. Rothaeusler K, Baumgarth N. B-cell fate decisions following influenza virus infection. European Journal of Immunology. 2010; 40:366–77. [PubMed: 19946883]
64. Baumgarth N, Herman OC, Jager GC, Brown LE, Herzenberg LA, Chen J. B-1 and B-2 cell-derived immunoglobulin M antibodies are nonredundant components of the protective response to influenza virus infection. The Journal of Experimental Medicine. 2000; 192:271–80. [PubMed: 10899913]
65. Ansel KM, Harris RB, Cyster JG. CXCL13 is required for B1 cell homing, natural antibody production, and body cavity immunity. Immunity. 2002; 16:67–76. [PubMed: 11825566]
66. Oliveira HC, Popi AF, Bachi AL, Nonogaki S, Lopes JD, Mariano M. B-1 cells modulate the kinetics of wound-healing process in mice. Immunobiology. 2010; 215:215–22. [PubMed: 19457571]

67. Parra D, Rieger AM, Li J, Zhang YA, Randall LM, Hunter CA, Barreda DR, Sunyer JO. Pivotal Advance: Peritoneal cavity B-1 B cells have phagocytic and microbicidal capacities and present phagocytosed antigen to CD4+ T cells. Journal of Leukocyte Biology. 2011; 91:525–36. [PubMed: 22058420]
68. Popi AF, Zamboni DS, Mortara RA, Mariano M. Microbicidal property of B1 cell derived mononuclear phagocyte. Immunobiology. 2009; 214:664–73. [PubMed: 19321225]
69. Pietrella D, Rachini A, Torosantucci A, Chiani P, Brown AJ, Bistoni F, Costantino P, Mosci P, d'Enfert C, Rappuoli R, Cassone A, Vecchiarelli A. A beta-glucan-conjugate vaccine and anti-beta-glucan antibodies are effective against murine vaginal candidiasis as assessed by a novel in vivo imaging technique. Vaccine. 2010; 28:1717–25. [PubMed: 20038431]
70. Alugupalli KR, Gerstein RM, Chen J, Szomolanyi-Tsuda E, Woodland RT, Leong JM. The resolution of relapsing fever borreliosis requires IgM and is concurrent with expansion of B1b lymphocytes. Journal of Immunology (Baltimore, Md : 1950). 2003; 170:3819–27.
71. Alugupalli KR, Leong JM, Woodland RT, Muramatsu M, Honjo T, Gerstein RM. B1b lymphocytes confer T cell-independent long-lasting immunity. Immunity. 2004; 21:379–90. [PubMed: 15357949]
72. Arjunaraja S, Massari P, Wetzler LM, Lees A, Colino J, Snapper CM. The nature of an in vivo anti-capsular polysaccharide response is markedly influenced by the composition and/or architecture of the bacterial subcapsular domain. J Immunol. 2012; 188:569–577. [PubMed: 22156342]
73. Colino J, Duke L, Arjunaraja S, Chen Q, Liu L, Lucas AH, Snapper CM. Differential idiotype utilization for the in vivo type 14 capsular polysaccharide-specific Ig responses to intact Streptococcus pneumoniae versus a pneumococcal conjugate vaccine. J Immunol. 2012; 189:575–586. [PubMed: 22706079]
74. Seidl KJ, MacKenzie JD, Wang D, Kantor AB, Kabat EA, Herzenberg LA, Herzenberg LA. Frequent occurrence of identical heavy and light chain Ig rearrangements. International Immunology. 1997; 9:689–702. [PubMed: 9184914]
75. Hardy RR, Carmack CE, Shinton SA, Riblet RJ, Hayakawa K. A single VH gene is utilized predominantly in anti-BrMRBC hybridomas derived from purified Ly-1 B cells. Definition of the VH11 family. Journal of Immunology (Baltimore, Md : 1950). 1989; 142:3643–51.
76. Mercolino TJ, Locke AL, Afshari A, Sasser D, Travis WW, Arnold LW, Haughton G. Restricted immunoglobulin variable region gene usage by normal Ly-1 (CD5+) B cells that recognize phosphatidyl choline. The Journal of Experimental Medicine. 1989; 169:1869–77. [PubMed: 2499651]
77. Oliveira DL, Nimrichter L, Miranda K, Frases S, Faull KF, Casadevall A, Rodrigues ML. Cryptococcus neoformans cryoultramicrotomy and vesicle fractionation reveals an intimate association between membrane lipids and glucuronoxylomannan. Fungal Genet Biol. 2009; 46:956–963. [PubMed: 19747978]
78. Yoshikawa S, Kawano Y, Minegishi Y, Karasuyama H. The skewed heavy-chain repertoire in peritoneal B-1 cells is predetermined by the selection via pre-B cell receptor during B cell ontogeny in the fetal liver. International Immunology. 2009; 21:43–52. [PubMed: 19011159]
79. Chattopadhyay G, Chen Q, Colino J, Lees A, Snapper CM. Intact bacteria inhibit the induction of humoral immune responses to bacterial-derived and heterologous soluble T cell-dependent antigens. J Immunol. 2009; 182:2011–2019. [PubMed: 19201854]
80. Nicola AM, Frases S, Casadevall A. Lipophilic dye staining of Cryptococcus neoformans extracellular vesicles and capsule. Eukaryotic Cell. 2009; 8:1373–80. [PubMed: 19465562]
81. Silverman GJ, Cary SP, Dwyer DC, Luo L, Wagenknecht R, Curtiss VE. A B cell superantigen-induced persistent "Hole" in the B-1 repertoire. The Journal of Experimental Medicine. 2000; 192:87–98. [PubMed: 10880529]
82. Foote JB, Kearney JF. Generation of B cell memory to the bacterial polysaccharide alpha-1,3 dextran. Journal of Immunology (Baltimore, Md : 1950). 2009; 183:6359–68.
83. Reese AJ, Doering TL. Cell wall alpha-1,3-glucan is required to anchor the Cryptococcus neoformans capsule. Molecular Microbiology. 2003; 50:1401–9. [PubMed: 14622425]

84. Reese AJ, Yoneda A, Breger JA, Beauvais A, Liu H, Griffith CL, Bose I, Kim MJ, Skau C, Yang S, Sefko JA, Osumi M, Latge JP, Mylonakis E, Doering TL. Loss of cell wall alpha(1–3) glucan affects Cryptococcus neoformans from ultrastructure to virulence. Molecular Microbiology. 2007; 63:1385–98. [PubMed: 17244196]

85. Xu JL, Davis MM. Diversity in the CDR3 region of V(H) is sufficient for most antibody specificities. Immunity. 2000; 13:37–45. [PubMed: 10933393]

86. Ippolito GC, Schelonka RL, Zemlin M III, Kobayashi R, Zemlin C, Gartland GL, Nitschke L, Pelkonen J, Fujihashi K, Rajewsky K, SHW. Forced usage of positively charged amino acids in immunoglobulin CDR-H3 impairs B cell development and antibody production. The Journal of Experimental Medicine. 2006; 203:1567–78. [PubMed: 16754718]

87. Schelonka RL III, Zhuang Y, Gartland GL, Zemlin M, SHW. Development of the expressed Ig CDR-H3 repertoire is marked by focusing of constraints in length, amino acid use, and charge that are first established in early B cell progenitors. Journal of Immunology (Baltimore, Md : 1950). 2005; 174:7773–80.

88. Mahmoud TI, SHW, Kearney JF. Limiting CDR-H3 diversity abrogates the antibody response to the bacterial polysaccharide alpha 1-->3 dextran. Journal of Immunology (Baltimore, Md : 1950). 2011; 187:879–86.

89. Mahmoud TI, Kearney JF. Terminal deoxynucleotidyl transferase is required for an optimal response to the polysaccharide alpha-1,3 dextran. Journal of Immunology (Baltimore, Md : 1950). 2010; 184:851–8.

90. Casadevall A, Scharff MD. The mouse antibody response to infection with Cryptococcus neoformans: VH and VL usage in polysaccharide binding antibodies. The Journal of Experimental Medicine. 1991; 174:151–60. [PubMed: 1676047]

91. Yang Y, Ghosn EE, Cole LE, Obukhanych TV, Sadate-Ngatchou P, Vogel SN, Herzenberg LA, Herzenberg LA. Antigen-specific antibody responses in B-1a and their relationship to natural immunity. Proc Natl Acad Sci U S A. 2012; 109:5382–5387. [PubMed: 22421134]

92. Yang Y, Ghosn EE, Cole LE, Obukhanych TV, Sadate-Ngatchou P, Vogel SN, Herzenberg LA, Herzenberg LA. Antigen-specific memory in B-1a and its relationship to natural immunity. Proc Natl Acad Sci U S A. 2012; 109:5388–5393. [PubMed: 22421135]

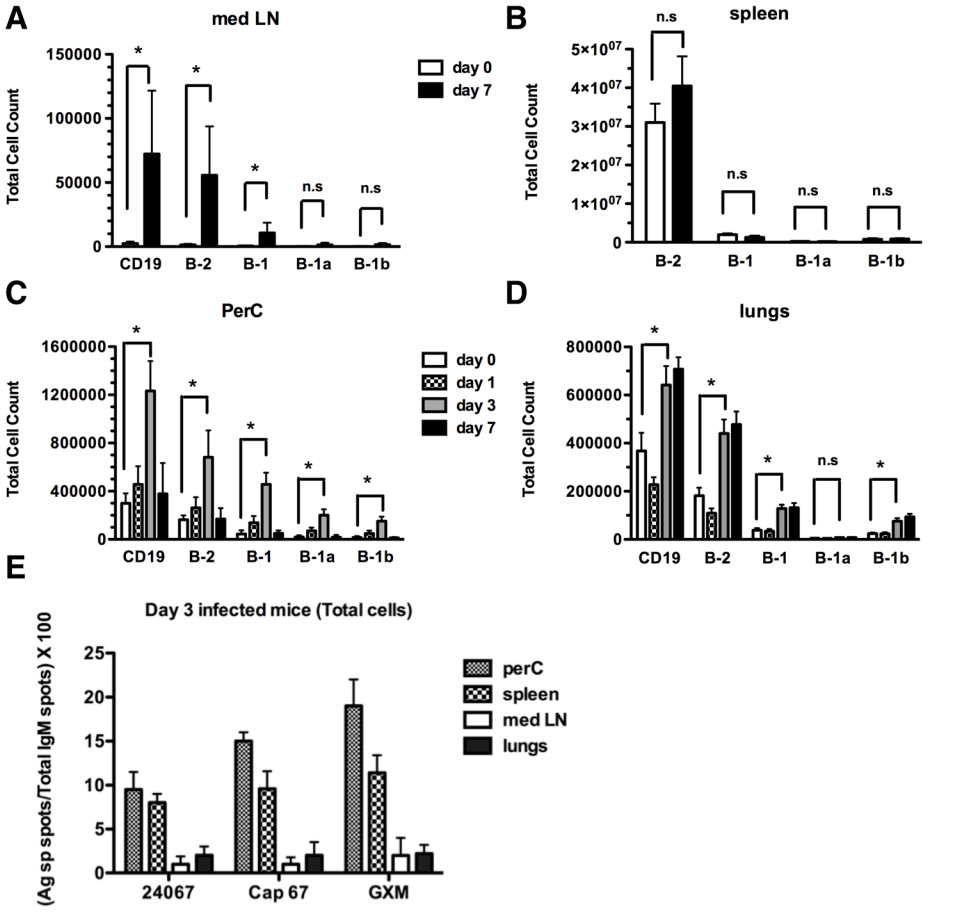

Figure 1.

B cell composition of medLN (A), spleen (B), PerC (C) and lungs (D) in CN-infected mice. The y-axis represents total cell number at the post-infection times on x-axis. Bars represent mean results ± standard errors of means (n=5 mice per group). P values calculated using Student's t test, comparing B cell populations in day 7 CN-infected with naïve mice (1A and B) and day 3 CN-infected with naïve mice (1C and D). * - $p<0.05$; n.s - not significant. (E) ELISPOT detection of IgM-producing CN antigen (shown on x axis)-binding B cells in day 3 CN-infected mice (n=5). Histograms depict percentage of B cells secreting CN antigen-binding IgM to total B cells secreting IgM.

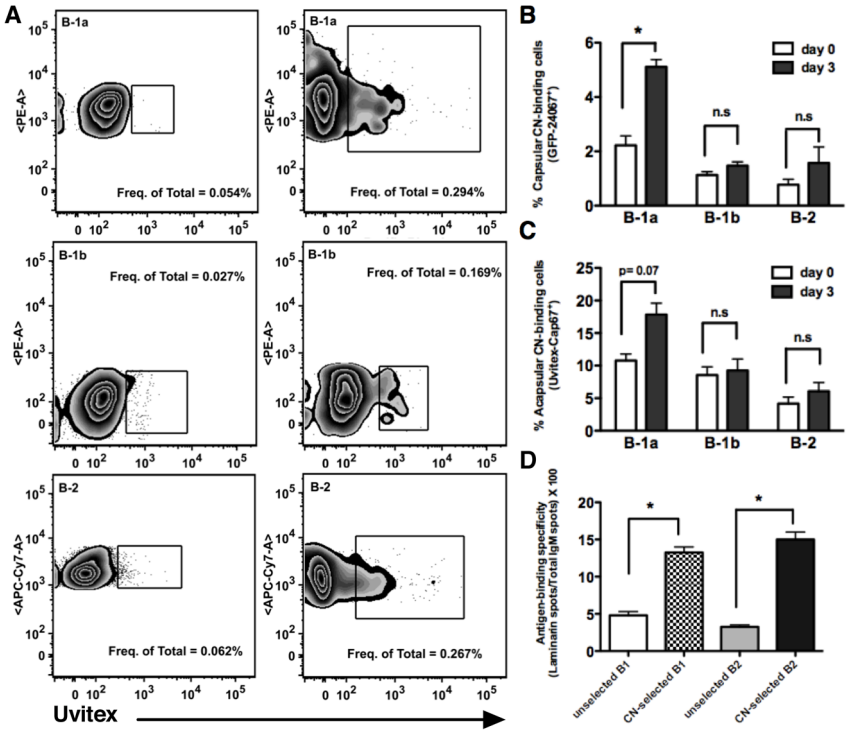

Figure 2.

Staining strategy for isolation of CN-selected and unselected B-1a, B-1b and B-2 cells. (A) Cells were stained with Uvitex-Cap67 and fluorescent antibodies recognizing B cell surface antigens. Gating strategy for B-1a cells (PE-CD5$^+$), B-1b cells (PE-CD5$^-$) and B-2 cells (APC-Cy7-B220$^+$) is shown; boxed population contains B cells that bind Uvitex-Cap67. The proportion of the total peritoneal B cell population represented within this gate is indicated for naïve mice (left panels) and day 3 CN-infected mice (right panels). Peritoneal cells were pooled from naïve and infected mice for identifying CN-binding cells (n=5 per group). Results shown are representative of three independent experiments. A similar strategy was used for identifying GFP-24067$^+$ B cells (data not shown). The fraction of (B) capsular CN-(GFP-24067$^+$)-binding B cells, and (C) acapsular CN-(Uvitex-Cap67$^+$) binding B cells is depicted for pooled peritoneal cells in naïve (open bars) and day 3 CN-infected (filled bars) mice (n=5 per group). The fractions were obtained from 3 independent experiments. (D) ELISPOT for B-1 and B-2 cells producing cryptococcal antigen-binding IgM following Uvitex-Cap67 selection. Cells were pooled from day 3 CN-infected mice (n=10). Antigen-binding specificity for unselected and CN-selected B-1 and B-2 populations is depicted as a percentage of the total number of laminarin-binding IgM spots/total number of IgM spots. * - $p<0.05$; Student t test.

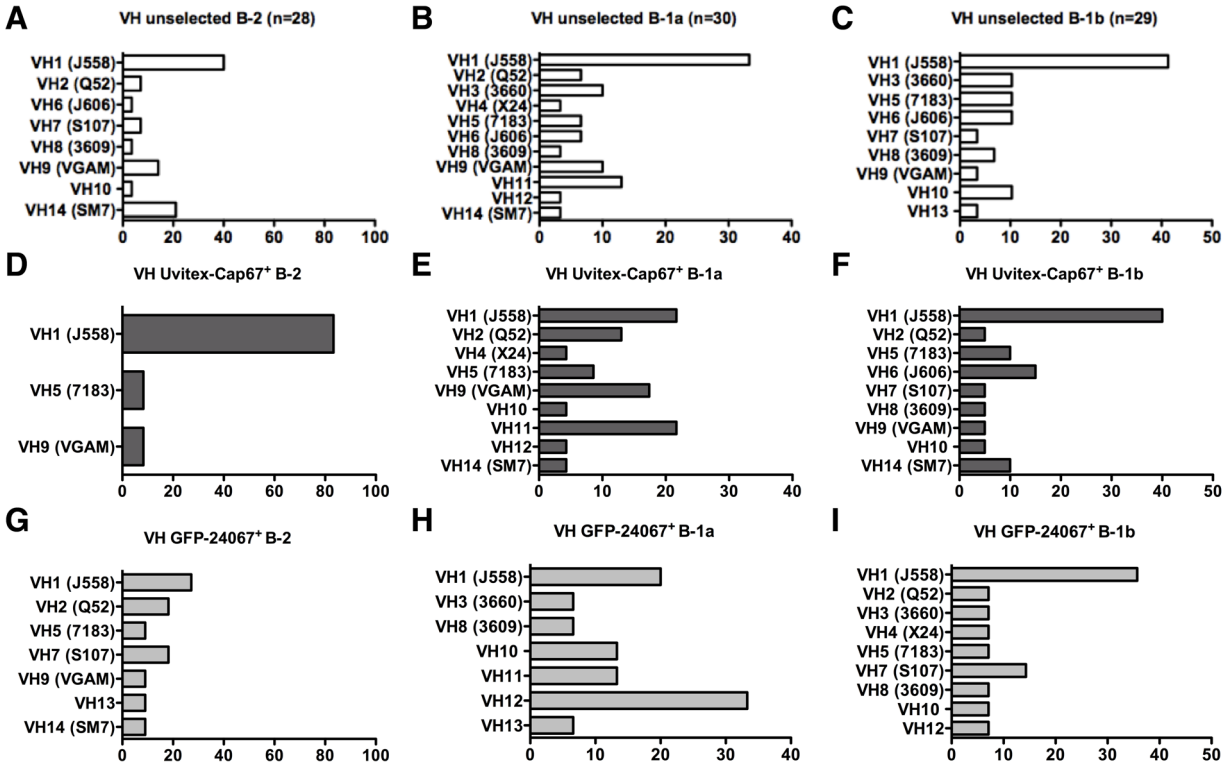

Figure 3.

IgV_H gene family usage. The V_H families used in unselected peritoneal B-2, B-1a and B-1b cells are presented (as percentage) in 3A, 3B and 3C respectively. Histograms depict V_H usage for acapsular CN-(Uvitex-Cap67$^+$) binding B-2, B-1a and B-1b cells in 3D, 3E, and 3F, respectively, obtained 3 days after CN infection. Figures 3G, 3H and 3I depict V_H usage in capsular CN-(GFP-24067$^+$) binding B-2, B-1a and B-1b cells, respectively. Data are from two independent experiments each using 10 mice.

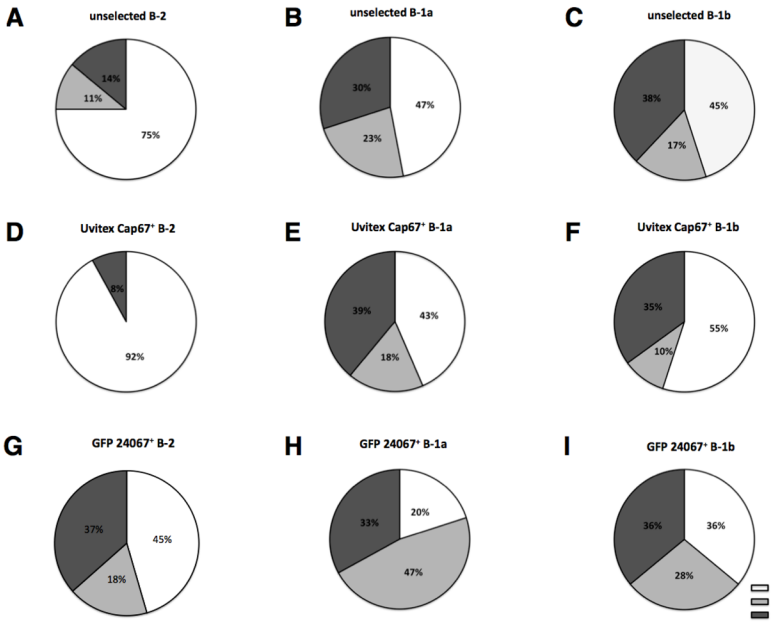

Figure 4.

Pie charts depicting V_H clan frequencies in unselected, acapsular CN-(Uvitex-Cap67$^+$), and capsular CN-(GFP-24067$^+$) binding B-2, B-1a and B-1b subsets. Clan I (V_H1, 9, 14 and 15) is shown in white, clan II (V_H2, 3, 8 and 12) in grey, and clan III (V_H4, 5, 6, 7,10, 11, 13 and 16) in black.

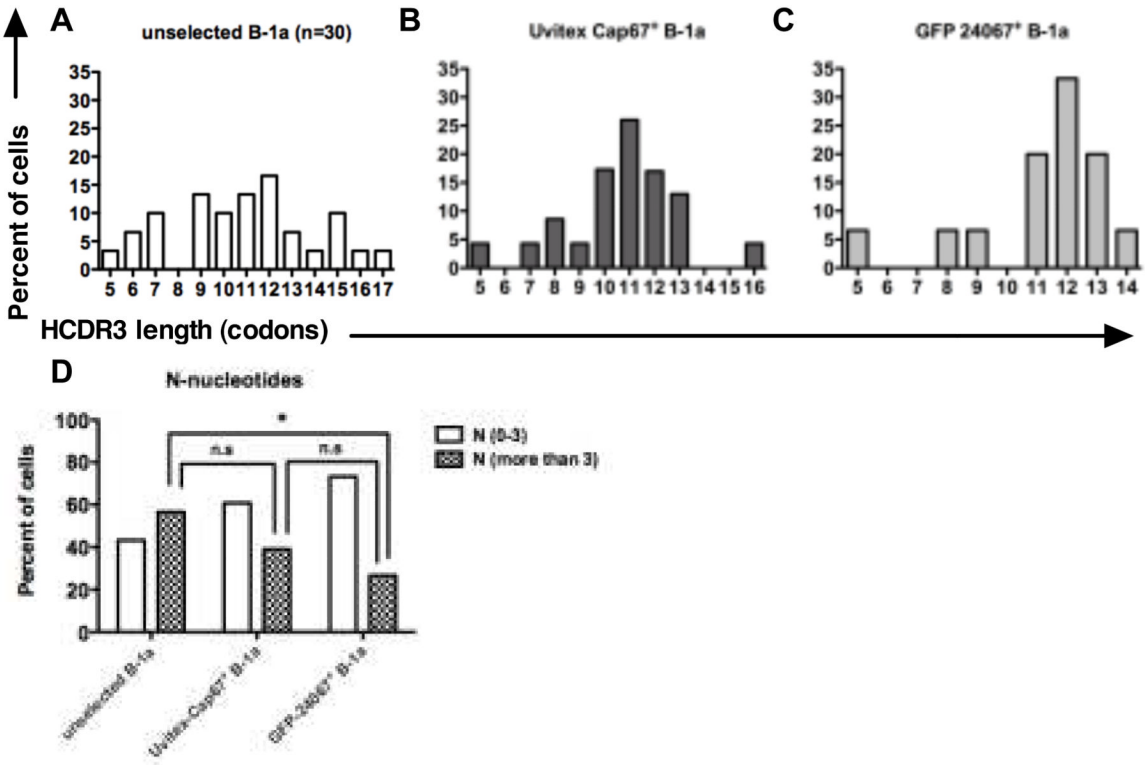

Figure 5.

The frequency of HCDR3 lengths is plotted (as percentage) for unselected, acapsular CN-(Uvitex-Cap67^{+}), and capsular CN-(GFP-24067^{+}) binding PerC B-1a cell subsets in 5A, 5B and 5C, respectively. HCDR3 was identified as the region between (but not including) the 3′ V_H encoded conserved cysteine (TGT) at Kabat position 92 and the 5′ J_H encoded conserved tryptophan (TGG) at Kabat position 103. (D) Comparison of N nucleotide addition among B-1a populations at both V_H-D_H and D_H-J_H junctions. * - $p<0.05$, n.s - not significant; Student t test.

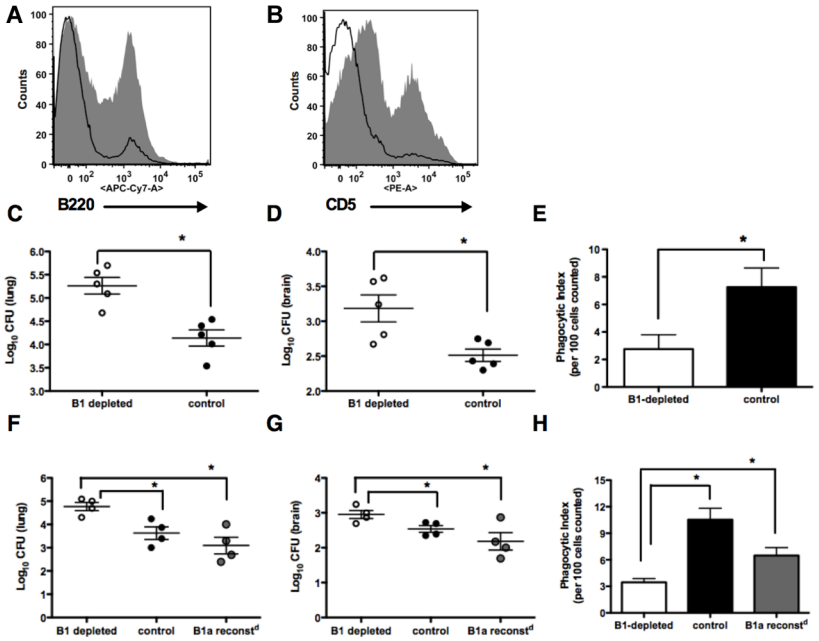

Figure 6.

B-1 cell depletion and reconstitution in C57Bl/6 mice. (A) FACS analysis of PerC $B220^+$ cells in mice treated with ddH_2O (dark line) compared with control (PBS) treated mice (shaded plot). (B) $CD5^+$ cells in PerC. (C) Lung and (D) Brain CFU in CN-infected control mice and B-1 depleted mice on day 3 post-infection (n=5 mice per group). (E) Phagocytic index (PI) for B-1 depleted mice and controls on day 3 post CN infection. (F) Lung and (G) Brain CFU in CN-infected control mice (not depleted, black circles), and B-1 depleted mice which were *(i)* reconstituted with B-1a cells (grey circles) and *(ii)* not reconstituted (open circles) on day 3 post-infection (n=4 mice per group). (H) Phagocytic index of alveolar macrophages from CN-infected controls, B-1 depleted, and B-1a reconstituted mice on day 3 post-infection. * - $p<0.05$; Students *t* test.